COO-535-649

EXCITATION ENERGIES OF LEVELS IN ^{16}F, ^{20}Na, AND ^{24}Al†

C. E. Moss* and A. B. Comiter††

Nuclear Physics Laboratory
Department of Physics and Astrophysics
University of Colorado
Boulder, Colorado 80302 USA

Abstract: Neutron time-of-flight spectra from the reactions $^{16}O(p,n)^{16}F$, $^{20}Ne(p,n)^{20}Na$, and $^{24}Mg(p,n)^{24}Al$ at E_p=23 MeV were used to locate levels in ^{16}F, ^{20}Na, and ^{24}Al. The excitation energies are compared with previously reported values and with the predictions from Coulomb displacement calculations.

E NUCLEAR REACTIONS ^{16}O, ^{20}Ne, $^{24}Mg(p,n)$, E=23 MeV; measured E_n. ^{16}F, ^{20}Na, ^{24}Al deduced levels. Natural and enriched targets.

† Work supported in part by the U. S. Atomic Energy Commission

* Present address: Research School of Physical Sciences, Australian National University, Canberra

†† Present address: California Institute of the Arts, Valencia, California

DISCLAIMER

1. Introduction

The information on the A=4n, T_z=-1 nuclei in the sd shell is very meager[1,2] because of the difficulties in reaching these nuclei. They are most easily produced with the reactions (p,n) or (^{3}He,t) for which the Q-values are ~ -15 MeV. There exists considerably more information on the analogue T_z=+1 nuclei. Information on the T_z=-1 nuclei is needed, for example, for studying Coulomb displacement energies between analogue levels and for searching for T_z=-2 nuclei by looking for their decays to the T_z=-1 nuclei.

2. Experimental procedure

A beam of ~800 nA of 22.9 MeV protons from the University of Colorado cyclotron bombarded the target which was mounted in a thin-wall Al target chamber. A positively biased grid was used in the ion source[3] to suppress all except every fourth, or every eighth, beam burst. On the fourth, or eighth, burst the grid was pulsed negatively to emit beam. The beam pipe near the target was 15 cm in diameter to minimize background from beam hitting the beam pipe. The beam was stopped ~1 m from the target in a Faraday cup shielded from the detector by ~10 cm of Fe shot and a brass shadow bar 30 cm (length) x 15 cm (diameter). Steel plates with an effective thickness of 15 to 45 cm depending on the detector angle were stacked near the target on the detector side to shield against neutrons and γ-rays from the beam pipe. A small opening (less than 10 cm x 10 cm) was left for the neutrons from the target.

The neutrons were detected in a 2.5 cm (thickness) x 14.0 cm (diameter) NE 224 scintillator, and γ-rays were rejected with n-γ pulse shape discrimination. For short (< 10 m) measurements, the scintillator was mounted at the back of a brass pipe 1.5 m (length) x 20 cm (diameter) which was surrounded by ~15 cm of Fe shot and 20 cm of paraffin. For long flight path (> 25 m) measurements,

two windows were cut in the walls of the target room at 17° and 50°, and the scintillator was mounted on a 5 m tower mounted on a flat bed truck which could be moved from one observation station to the other. The scintillator was shielded by ~15 cm of paraffin, except for an opening for the neutrons from the target, and a paraffin and Fe shot collimator was placed at ~8 m. Other than what has already been mentioned, no other shielding was used in the target area for any of the measurements. The walls and floor of the target room were thin and caused very little neutron back-scattering.

The contribution to the time resolution from the detector system was 0.8 ns (FWHM) and from the cyclotron, 0.3 ns (FWHM). The contribution from the finite target thickness depended on the flight path. For the long flight path measurements the total energy resolution was typically 40 keV (FWHM) for 6 MeV neutrons and was limited mainly by the target thickness. Of course, thinner targets and longer flight paths would have given better energy resolution but required longer measurements. The measurements with short flight paths took ~12 hours while those with short flight paths took ~1 hour.

The Mg target contained 99.96% Mg and was 2.6 mg/cm^2 thick. For Ne and O_2, two different gas cells were used. A gas cell 2.54 cm (length) x 1.27 cm (diameter) with 0.86 mg/cm^2 natural Ni windows on each end was used to retain ~0.2 atm of natural Ne and natural O_2 for the short flight path measurements. A gas cell 6.6 cm in diameter with a 2.7 mg/cm^2 mylar foil around most of the circumference retained ~0.2 atm of the same gases for the long flight measurements. It was necessary to rotate this second cell so that the beam was incident at a different spot on the window approximately every 30 min. to keep the beam from puncturing the mylar windows. In addition, the current in a small steering magnet upstream from the target was modulated with a triangular waveform at a frequency of 1 Hz to sweep the beam over a distance of ~3 mm. The mylar

windows had the advantage that they produced very little background, whereas the Ni windows had the advantage that they lasted many hours without special precautions.

The incident beam energies for the various measurements were determined in two ways. First, the energies were determined from an NMR measurement of the field of a beam analyzing magnet which had been calibrated with a charged particle time-of-flight system[4]). Second, the energies were calculated from the separations in the time spectra of peaks from levels with well-known excitation energies in other nuclei which were studied at the same time. For example, the separation between the peaks corresponding to the g.s. and the 937.2±0.5 keV level[5]) in ^{54}Co formed by the reaction ^{54}Fe(p,n)^{54}Co was used. For each series of measurements, an average of the various beam energy determinations was taken and a standard deviation calculated. In calculating the beam energies and in calculating the excitation energies from the time spectra appropriate energy loss corrections were made[6,7]). All of the peaks used to determine the beam energies and also those used to calculate excitation energies were fitted with Gaussian shapes. The computer program SPECTR[8]) which can fit several overlapping peaks was used.

3. Results

The data for the three reactions ^{16}O(p,n)^{16}F, ^{20}Ne(p,n)^{20}Na, and ^{24}Mg(p,n)^{24}Al studied here consist of long flight path spectra at 17° and 50° and short flight spectra at 20 angles between 10° and 150°. The angular distributions will be presented in a separate report on an extensive study of (p,n) angular distributions from 35 different targets[9]).

3.1. THE NUCLEUS ^{16}F

High resolution spectra were taken at 17.4° and 49.5° with flight paths of 26.04 m and 30.75 m, respectively. A short flight path spectrum taken at

31.1° is shown in fig. 1. The ground state and first excited state are weakly populated whereas the second and third are strongly populated. Excitation energies from the present work and previous work are given in table 1. The value for the excitation energy of the first excited state given in ref. [10]) is considerably higher than that obtained in the present work.

3.2. THE NUCLEUS ^{20}Na

High resolution spectra were taken at 17.4° and 49.5° with flight paths of 26.04 and 30.75 m, respectively. A short flight path spectrum taken at 60.7° is shown in fig. 2. The excitation energies are summarized in table 2. In none of the spectra was there any convincing evidence of a state at .85 MeV as reported in ref. [13]). Instead the fourth level in the quartet expected from the mirror nucleus ^{20}F (see fig. 5) is tentatively placed at 1010±14 keV. This level was not resolved in the short flight path measurements and was weakly populated at the two angles used for the long flight path measurements. The excitation energy of the first excited state given in ref. [13]) is considerably higher than that obtained in the present work.

3.3. THE NUCLEUS ^{24}Al

The two long flight path spectra are shown in fig. 3. The fact that the yield for the 441 keV state is low at 50° is consistent with a $J^{\pi}=1^{+}$ assignment[14]) for the state. Excitation energies from the present work and previous work are given in table 3. Two doublets (.441-.514, 1.578-1.651) clearly resolved here were not resolved in ref. [15]). The excitation energy of 441 ± 5 keV for the first excited state is in excellent agreement with the more accurate value of 439 ± 2 keV from a Ge(Li) measurement reported in ref. [14]).

4. Discussion

Figs. 4-6 show the isobaric level diagrams for A-16, 20, and 24, respectively, and table 4 compares the experimental excitation energies with those based on a

recent calculation[23]) of Coulomb displacement energies. The correspondence between the experimental and calculated levels is only based on the excitation energies when definite J^{π} assignments have not been made. For A=16, the ordering of the levels is not the same in the three members of the triplet. The J^{π} assignments are well established for the T=1 levels in ^{16}N and ^{16}O. However, in ^{16}F there is some controversy. Using the 0^-, 1^-, 2^-, 3^- ordering suggested in ref. [13]), we obtained satisfactory agreement with the calculations. Using the ordering suggested in ref. [11]) would have resulted in poor agreement.

For ^{20}F and ^{20}Ne the information is not complete. Two of the first six T=1 states in ^{20}Ne have not been identified. The present results suggest that the orderings of the first three states in ^{20}F and ^{20}Na are the same because these three states are fairly well separated in excitation energy (fig. 5) and the experimental excitation energies are only in satisfactory agreement with the calculated values of ref. [23]) if the orderings are the same. Therefore the J^{π} values of the ground state, 591, and 768 keV levels in ^{20}Na are probably 2^+, 3^+, and 2^+, respectively. The 1310 keV level in ^{20}Na most probably corresponds to the 1309 keV level in ^{20}F and therefore has $J^{\pi}=1^+$. For the doublet at 1 MeV, the present data are not sufficient to establish if the ordering of the levels is the same in ^{20}F and ^{20}Na. Measurements of the branching ratios for these two levels in ^{20}Na might help since in ^{20}F the 984 keV level has a 10% branch to the first excited state while the 1057 keV level does not[16]).

For ^{24}Na and ^{24}Mg the information is also incomplete. Three of the first eight T=1 states in ^{24}Mg have not been identified. The present results suggest that the 514 keV level in ^{24}Al corresponds to the 563, $J^{\pi}=(2)^+$ level in ^{24}Na since the correspondences for the only other two levels below 1 MeV excitation energies are fairly well established (fig. 6) and the calculated values of ref. [23]) agree best with the experimental excitation energies under this assumption (table 4). With less certainty one can speculate that the weakly populated 1292 keV level corresponds to the 1511, $J^{\pi}=(5)^+$ level in ^{24}Na and that

the 1120 keV level in ^{24}Al is a close doublet.

We would like to thank the University of Colorado neutron time-of-flight group which includes Mr. R. F. Bentley, Mr. J. D. Carlson, Professor D. A. Lind, and Professor C. D. Zafiratos for the use of the time-of-flight facility and for extensive assistance in the acquisition and analysis of the data. We would also like to thank Dr. H. Rudolph for his assistance in the acquisition of the data and Mr. D. A. Becker for his excellent assistance in the data analysis.

References

1) F. Ajzenberg-Selove, Nucl. Phys. A166 (1971) 1

2) P. M. Endt and C. van der Leun, Nucl. Phys. A105 (1967) 1

3) R. F. Bentley, L. A. Erb, D. A. Lind, C. D. Zafiratos, and C. S. Zaidins, Nucl. Instr. and Meth. 83 (1970) 245

4) G. W. Edwards and W. R. Smythe, Bull. Am. Phys. Soc. 14 (1969) 1242

5) N. S. P. King, C. E. Moss, H. W. Baer, and R. A. Ristinen, submitted to Nuclear Physics

6) J. B. Marion and F. C. Young, Nuclear Reaction Analysis (North-Holland, Amsterdam, 1968)

7) C. Williamson and J. P. Boujot, Tables of Range and Rate of Energy Loss of Charged Particles of Energy 0.5 to 150 MeV (Centre d'Etudes Nucleaires de Saclay, 1962), unpublished

8) D. H. Zurstadt, private communication

9) R. F. Bentley, J. D. Carlson, D. A. Lind, R. B. Perkins, and C. D. Zafiratos, to be published

10) J. M. Adams, A. Adams, and J. M. Calvert, Phys. Soc. (London) J. Phys. A 1 (1968) 549

11) C. D. Zafiratos, F. Ajzenberg-Selove, and F. S. Dietrich, Phys. Rev. 137 (1965) B1479

12) P. F. Donovan and P. D. Parker, Phys. Rev. Lett. 14 (1965) 147

13) R. H. Pehl and J. Cerny, Phys. Lett. 14 (1965) 137

14) A. J. Armini, J. W. Sunier, R. M. Polichar, and J. R. Richardson, Phys. Lett. 21 (1966) 335

15) N. Mangelson, M. Reed, C. C. Lu, and F. Ajzenberg-Selove, Phys. Lett. 21 (1966) 661

16) P. A. Quin, G. A. Bissinger, and P. R. Chagnon, Nucl. Phys. A155 (1970) 495

17) T. Holtebekk, R. Strømme, and S. Tryti, Nucl. Phys. A142 (1970) 251

18) A. A. Rollefson, P. F. Jones, and R. J. Shea, Phys. Rev. C 1 (1970) 1761

19) B. T. Lawergren, A. T. G. Ferguson, and G. C. Morrison, Nucl. Phys. A108 (1968) 325

20) J. D. Pearson and R. H. Spear, Nucl. Phys. 54 (1964) 434

21) J. W. Sunier, A. J. Armini, R. M. Polichar, and J. R. Richardson, Phys. Rev. 163 (1967) 1091

22) E. Kramer, G. Mairle, and G. Kaschl, Nucl. Phys. A165 (1971) 353

23) R. J. DeMeijer, H. F. J. van Royen, and P. J. Brussaard, Nucl. Phys. A164 (1971) 11

Table 1

Excitation energies (MeV ± keV) in ^{16}F

(p,n) Present work	(^{3}He,t) ref. [10])	(^{3}He,t) ref. [11])
.197 ± 12	.253 ± 35	.20 ± 50
.424 ± 5	.422 ± 15	.436± 30
.720 ± 6	.711 ± 15	.736± 40

Table 2

Excitation energies (MeV ± keV) in ^{20}Na

(p,n) Present work	(^{3}He,t) ref. [12])	(^{3}He,t) ref. [13])
.591 ± 12		.65 ± 50
.768 ± 8	.76 ± 50	.75 ± 50
		.85 ± 50
.958 ± 8		.95 ± 50
(1.010 ± 14)		
1.310 ± 10	1.3 ± 100	1.27 ± 50

Table 3

Excitation energies (MeV ± keV) in ^{24}Al

(p,n) Present work	γ decay ref. [14])	(^{3}He,t) ref. [15])
.441 ± 5	.439 ± 2	
		.47 ± 30
.514 ± 5		
1.120 ± 9		1.12 ± 30
1.292 ± 7		1.28 ± 50
1.578 ±10		1.62 ± 40
1.651 ±13		

Table 4

Comparison of theoretical and experimental excitation energies (keV)

Nucleus	J^{π} a)	E_x^{calc} b)	E_x^{expt}	$E_x^{calc} - E_x^{expt}$
$^{16}_{F}$	0^-	20	0	20
	1^-	290	197	93
	2^-	400	424	-24
	3^-	680	720	-40
$^{20}_{Na}$	2^+	20	0	20
	3^+	560	591	-31
$^{24}_{Al}$	4^+	-66	0	-66
	1^+	383	441	58
	2^+	437	514	-77
	1^+	1170	1120	50

a) Theoretical values[23]). Experimental assignments are summarized in figs. 4-6.

b) Calculated from theoretical Coulomb displacement energies[23]).

Figure Captions

Fig. 1 Neutron time-of-flight spectrum from protons on an oxygen target with a flight path of 7.52 m.

Fig. 2 Neutron time-of-flight spectrum from protons on a neon target with a flight path of 8.28 m. The peak labelled "γ" is due to imperfect n-γ pulse shape discrimination. The yield from the tentative 1010 keV level is small at this angle.

Fig. 3 Neutron time-of-flight spectra from protons on an enriched ^{24}Mg target at 18.7° and 50.1°. The flight paths were 25.96 and 28.10 m.

Fig. 4 Isobaric level diagram for A=16. The information on ^{16}N, ^{16}O, and the spins in ^{16}F are taken from the literature[1]). The dashed lines indicate the suggested correspondences.

Fig. 5 Isobaric level diagram for A=20. The information on ^{20}F, ^{20}Ne, and the spins in ^{20}Na are taken from the literature[16-21]). The dashed lines indicate the suggested correspondences.

Fig. 6 Isobaric level diagram for A=24. The information on ^{24}Na, ^{24}Mg, and the spins in ^{24}Al are taken from the literature[2,19,22]). The dashed lines indicate the suggested correspondences.

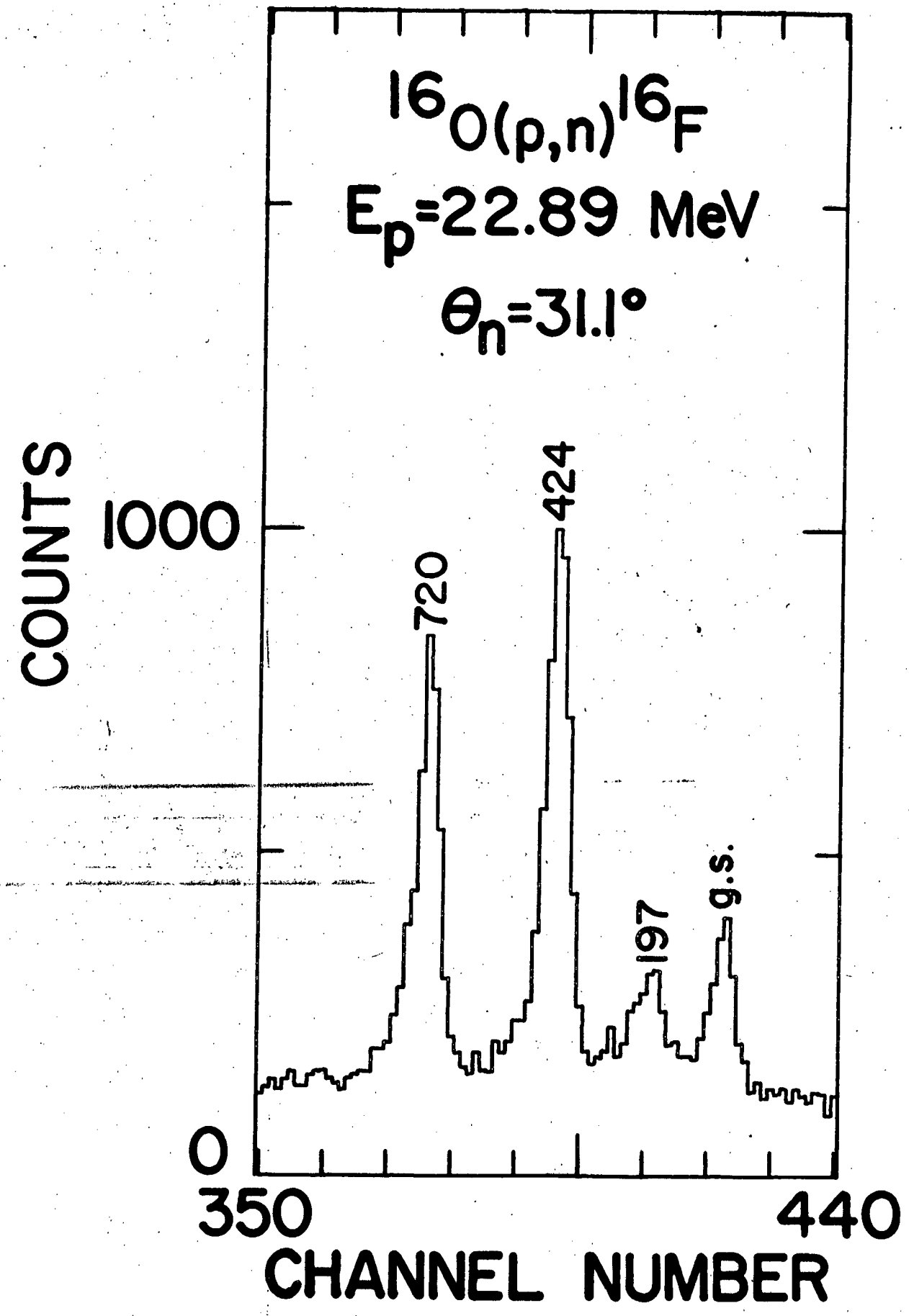
$^{16}O(p,n)^{16}F$
E_p=22.89 MeV
θ_n=31.1°
COUNTS
1000
0
720
424
197
g.s.
350
440
CHANNEL NUMBER

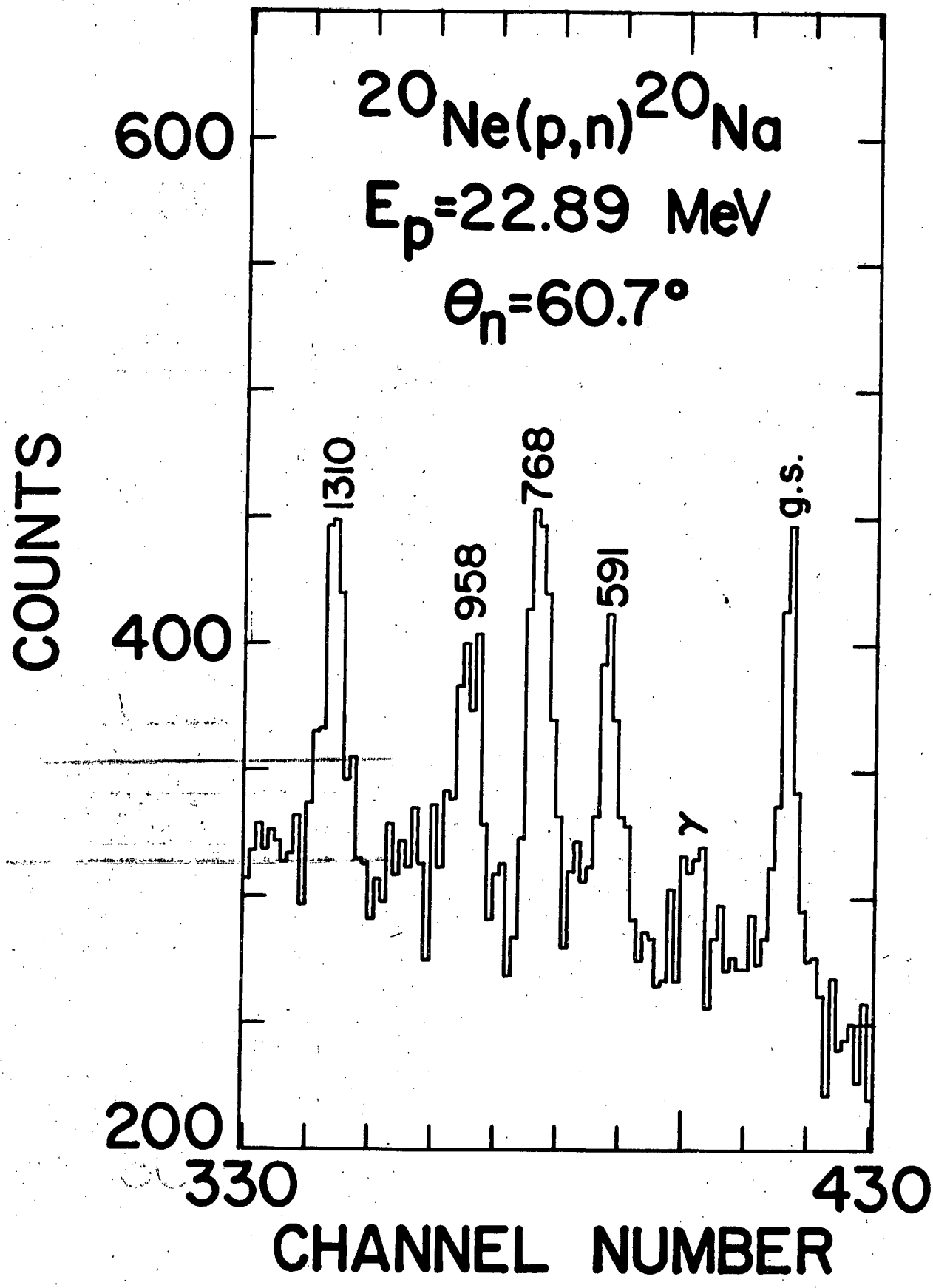
$^{20}Ne(p,n)^{20}Na$
E_p=22.89 MeV
θ_n=60.7°
600
400
200
COUNTS
1310
958
768
591
γ
g.s.
330
430
CHANNEL NUMBER

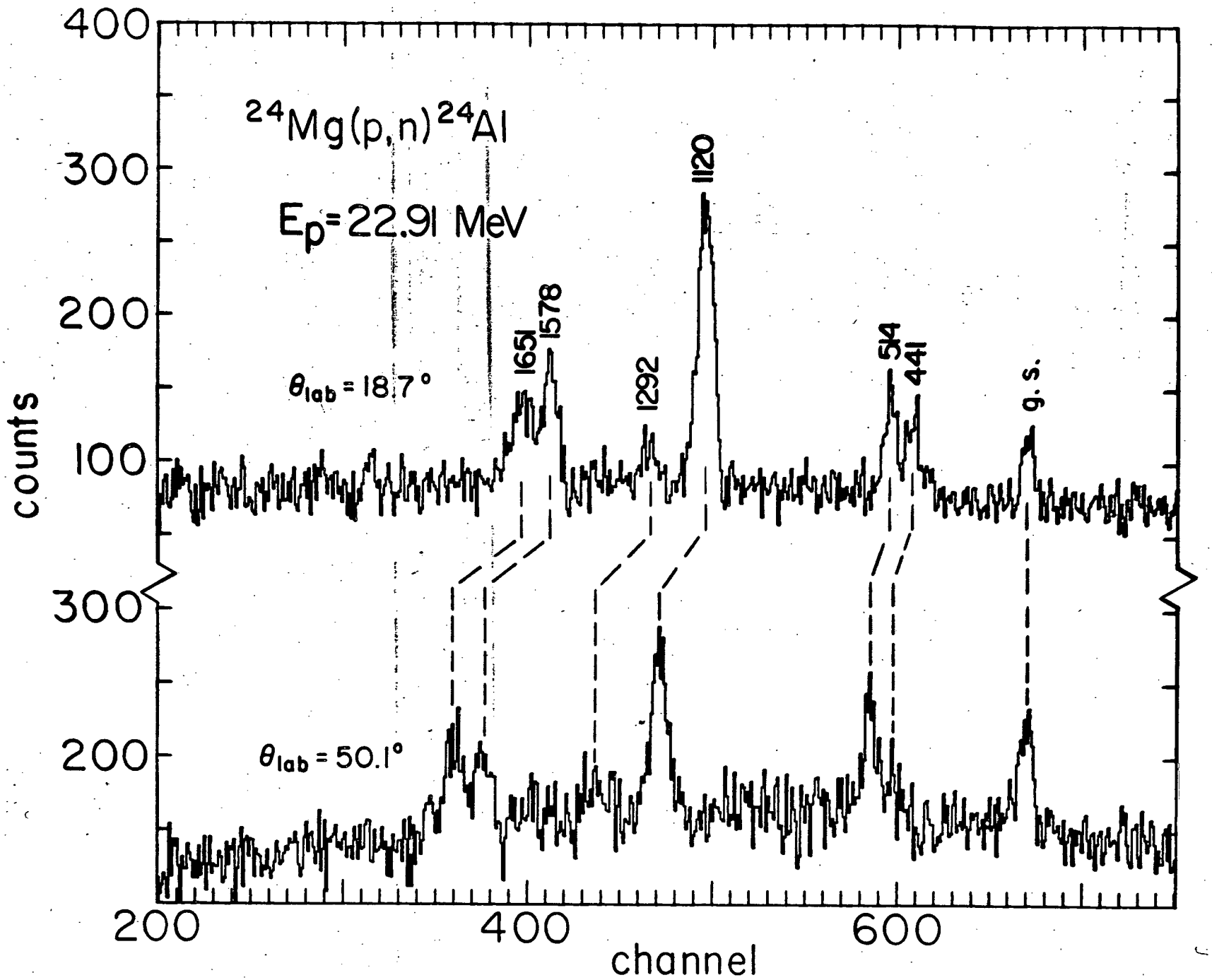
$^{24}Mg(p,n)^{24}Al$
E_p=22.91 MeV
θ_{lab} = 18.7°
θ_{lab} = 50.1°
1651
1578
1292
1120
514
441
g.s.
counts
channel
400
300
200
100
300
200
200
400
600

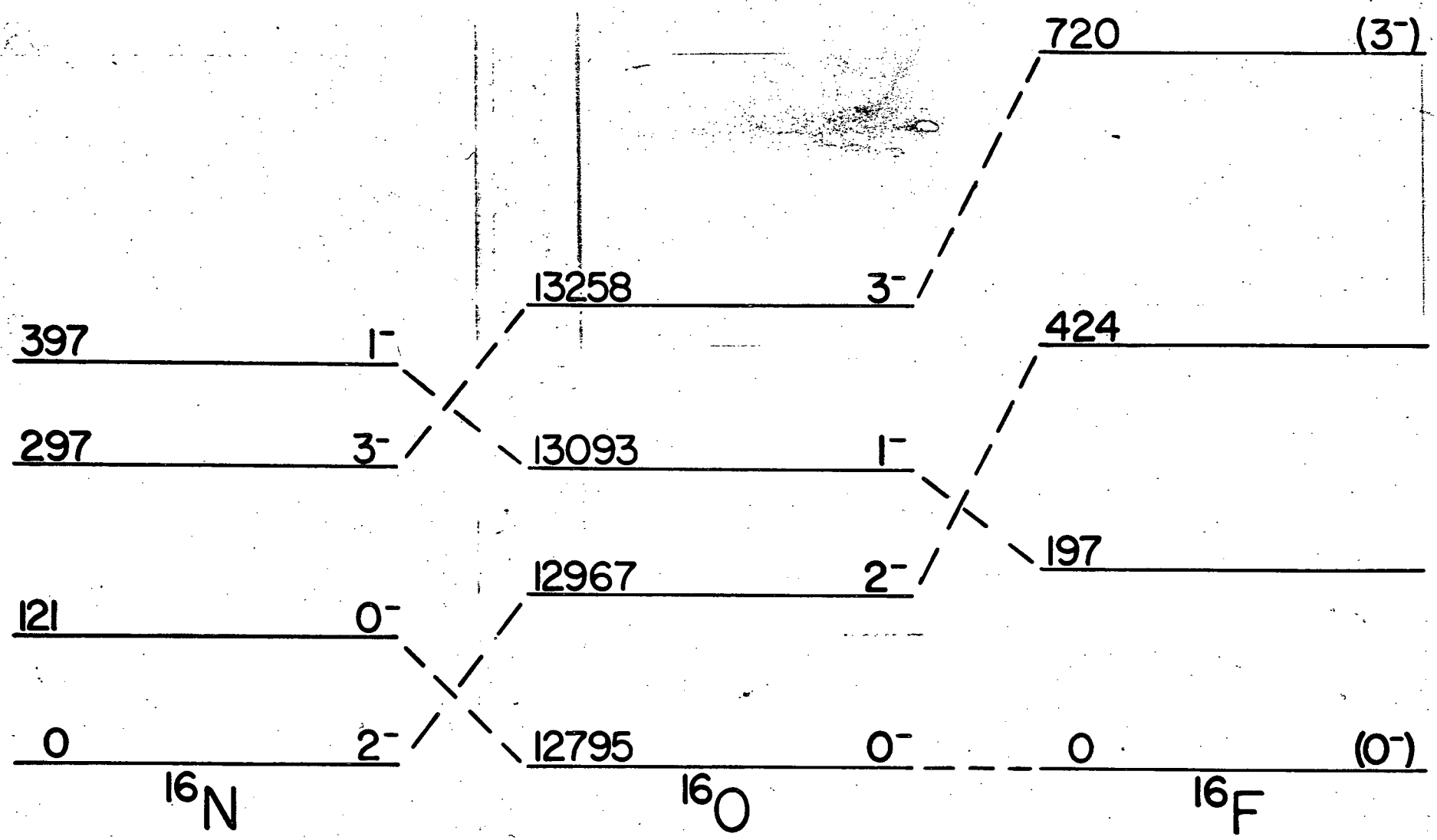
720
(3⁻)
13258
3⁻
397
1⁻
424
297
3⁻
13093
1⁻
197
12967
2⁻
121
0⁻
0
2⁻
12795
0⁻
0
(0⁻)
16N
16O
16F

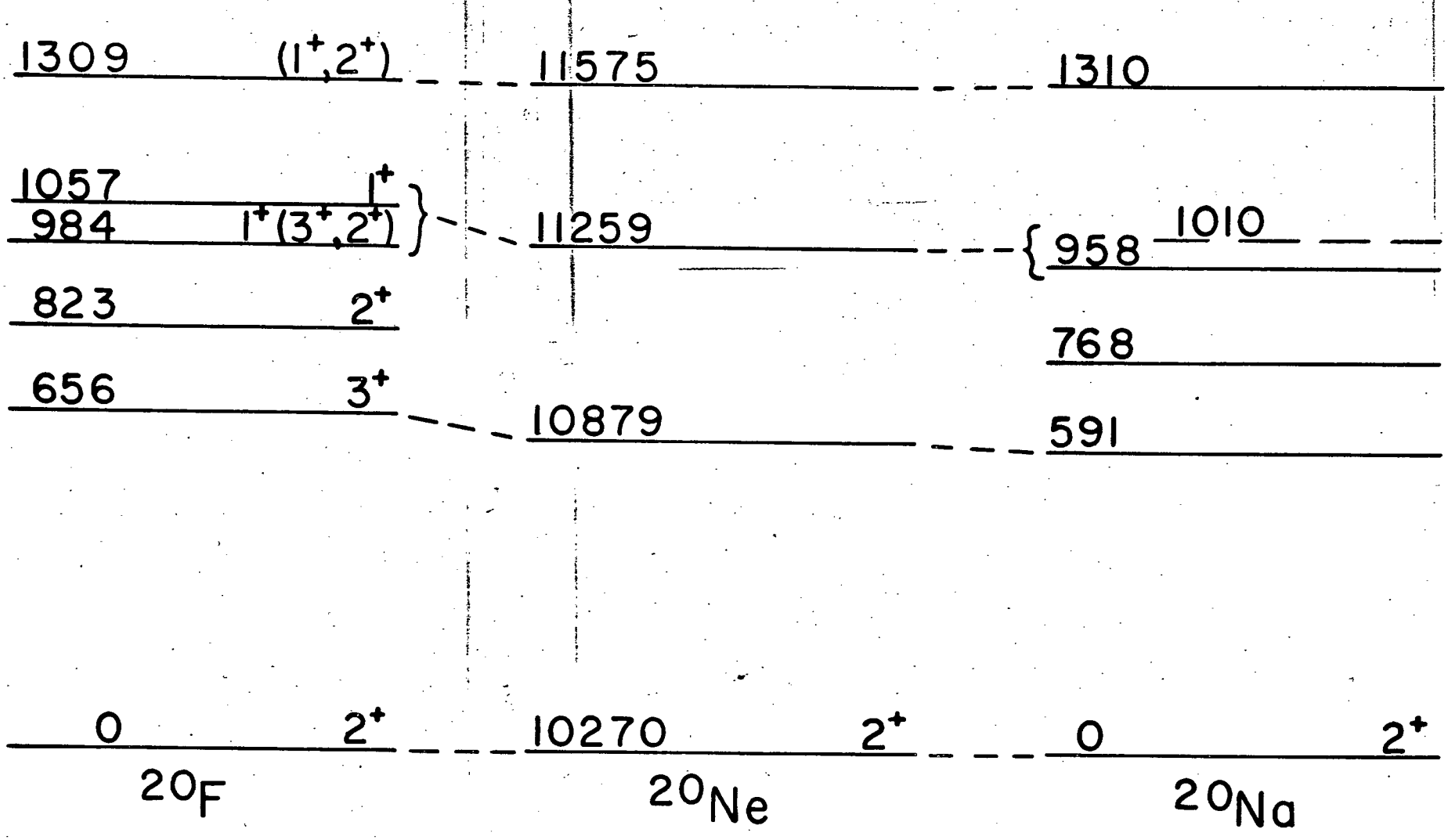
1309
(1+,2+)
11575
1310
1057
1+
984
1+(3+,2+)
11259
958
1010
823
2+
768
656
3+
10879
591
0
2+
10270
2+
0
2+
20F
20Ne
20Na

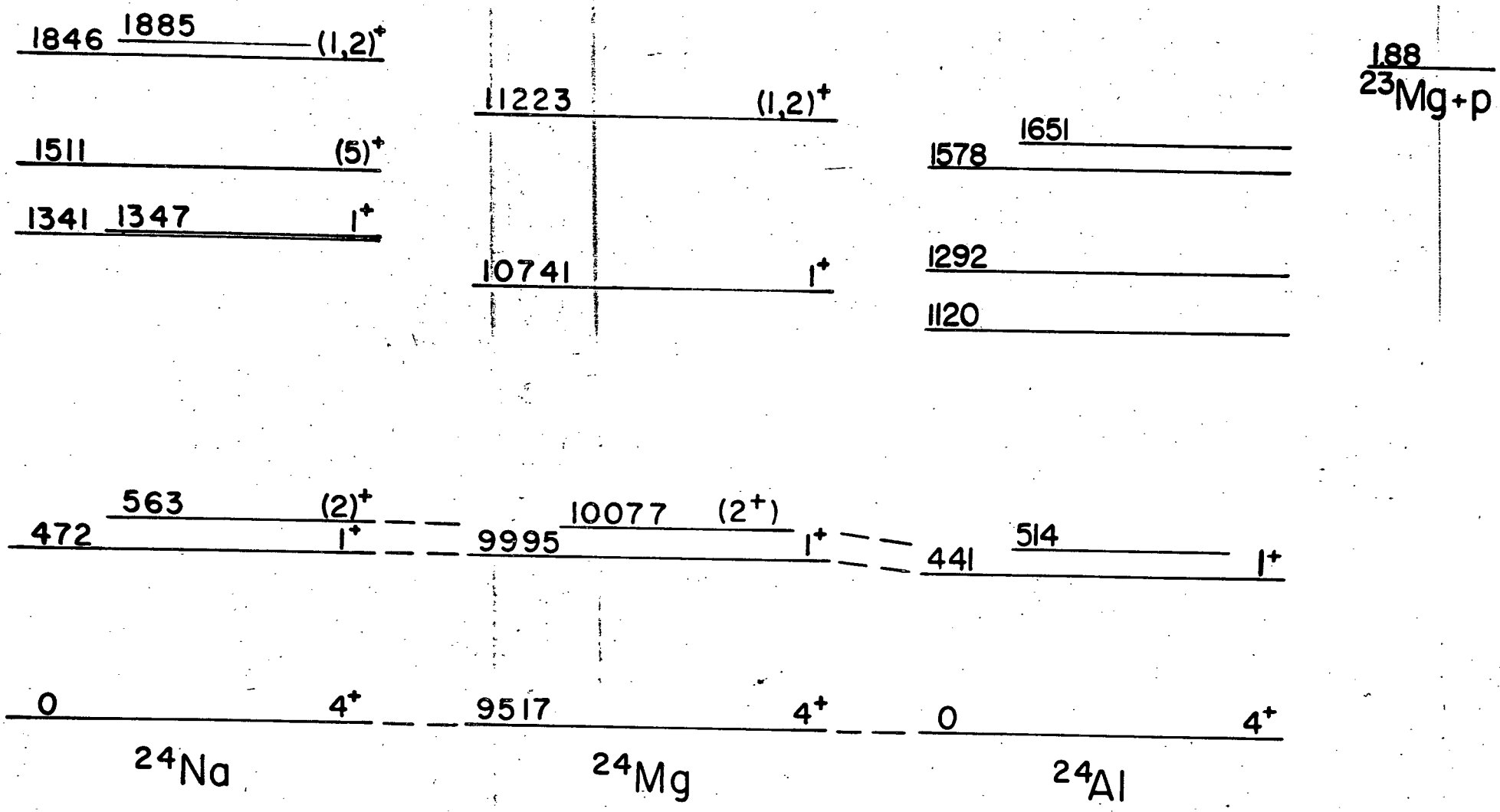
1846
1885
(1,2)+
1511
(5)+
1341
1347
1+
11223
(1,2)+
10741
1+
188
23Mg+p
1651
1578
1292
1120
563
(2)+
472
1+
10077
(2+)
9995
1+
514
441
1+
0
4+
9517
4+
0
4+
24Na
24Mg
24Al